Using a commercial mini-X-ray source for calibrating Bragg crystals

Published in:
Journal of Instrumentation

Document Version:
Peer reviewed version

Queen's University Belfast - Research Portal:
Link to publication record in Queen's University Belfast Research Portal

Using a commercial mini-x-ray source for calibrating Bragg crystals

F. Valle Brozas,[1] **C Hyland, S. White, S. Warnock, R. Irwin J. Campbell and D. Riley**

Centre for Plasma Physics, Queen's University Belfast,
University Road, Belfast BT7 1NN, UK

E-mail: f.vallebrozas@qub.ac.uk

ABSTRACT: In this paper we describe a procedure for calibration of Bragg crystals used for X-ray spectroscopy of laser plasmas. The method uses a relatively inexpensive commercially available X-ray source. By using the source to pump a metallic foil such as vanadium or titanium we were able to create a K-α emission source with minimal background radiation outside the desired photon energy. By using photon counting techniques with a CCD detector we were able to get absolute calibrations of curved and flat Bragg crystals in the 4-5 keV region. An important advantage of our method is that absolute calibration was not necessary either for the commercial source or the detector.

---

[1]Corresponding author.

Contents

---

1 Introduction

Bragg crystals are widely used in x-ray spectroscopy of plasmas for identifying X-ray lines generally in the 1-20 (roughly 0.5 -10 keV) range , e.g. [1–3]. As well as being used to identify information on electron temperature and density from line ratios and widths it is often desirable to measure the absolute number of photons emitted, especially in many laser-plasma experiments where X-rays are used to drive a plasma. The ability to readily obtain absolute calibration of integrated reflectivity of crystals with some reasonable accuracy is therefore useful but not always cheap or easy. In this paper we describe how we have achieved this with relatively inexpensive and easily used equipment for both flat and curved crystals.

2 Generation of a K-α source

The first part of the experiment was to generate a photon source with a narrow spectral range suitable for a photon counting experiment with a CCD detector. To do this we use a commercial x-ray source (Amptek, mini-X) with a Au cathode. With a maximum voltage of 50 kV this produces a spectrum of X-rays with photon energy up to 50 keV but with characteristic peaks due to the L-shell of Au in the 9-11 keV range. The beam is partially collimated and is specified to give 1.3×10^6 counts/sec/mm^2 at 30 cm from the cathode. The full specified x-ray beam parameters and spectrum can be obtained from the manufacturer. In figure

In the first stage of the calibration we placed the CCD 140 mm from a 10μm V foil with the Pb screen 70 mm in front of the source. The experiments need to be carried out with crystals set away from the main beam direction and so we wished to test the sensitivity to angle. Figure

In analysing this data we can see that the K-α peak stretches from around 100-150 counts/pixel due to the thermal width of the peak. However, as can be seen, this means that there is some merging at the lower end with the "split events" where the charge cloud created by an absorbed photon is shared between two or more adjacent pixels [4]. To account for this, after background subtraction (average of 160-180 counts/pixel range) we assume symmetry of the K-α peak and use the area under the peak from the maximum at 125 counts/pixel to 160 counts/pixel. Since this should include half of the K-α peak but most of the K-β peak, this means the we use a correction factor of $\sim (1 + 2\gamma_K)/2$ to approximately account for the latter. A more precise approach, that allows us to take account of the difference in filter transmission and quantum efficiency for the different photon energies, is described below for the crystal calibration work. In figure

The stability of the source is important in carrying out calibration work. To test this, we took data for a fixed CCD position every 15 minutes for over 2 hours. Each measurement consisted of 200 accumulations of 0.3s integration time and accumulated approximately 10^5 photons. We
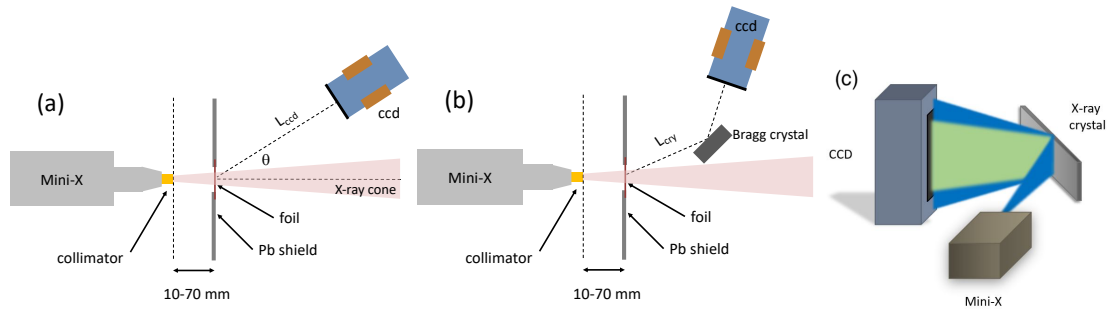
Figure 1. (a) Schematic of initial set up, not to scale. The Pb shield was 1.8 mm thick and had a 2 mm diameter aperture. The mini-X output was 70 mm from the aperture. The CCD detector used was an Andor DX420-BN with 1024 x 255 pixels of $26\mu m$ square. The peak quantum efficiency at 4-5 keV, supplied by the manufacturer ranged from 40-60%. (b) Schematic of set-up for crystal calibration. The crystal was positioned such that the direction to the crystal from the foil was the same as for the initial measurement of K-α photons in (a). In both cases the equipment was surrounded by a 0.9 m long x 0.7m wide x 0.3 m high enclosure made from 5mm thick Al and lined with 1.8mm Pb. The base was a steel table 1 cm thick. (c) Schematic of the arrangement with a flat crystal in place. The blue shading shows the angular spread limit imposed by the width of the crystal whilst, the green shading illustrates the case where it is the size of the chip that limits the angular spread.
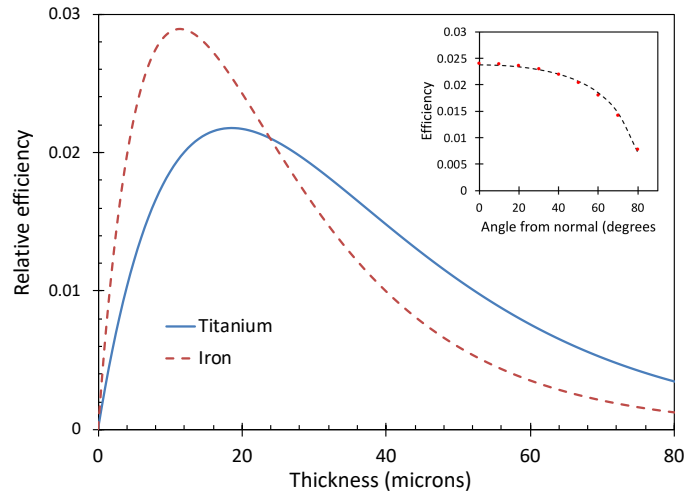
Figure 2. Relative efficiency of two different foils as a function of thickness. The emission is assumed to be along the normal to the foil and is expressed as a relative yield per sr per pump photon. The model integrates emission through the foil accounting for absorption of both the pump and emitted fluorescence. The inset shows calculations for 10 μm V foils as a function of angle (red circles). The dashed curve in the inset shows how we can represent the calculated emission with a simple function of form $I=A\exp(-\tau_0/\cos(\theta))$, where τ_0=0.25, which represents an effective average opacity for observation at normal incidence.
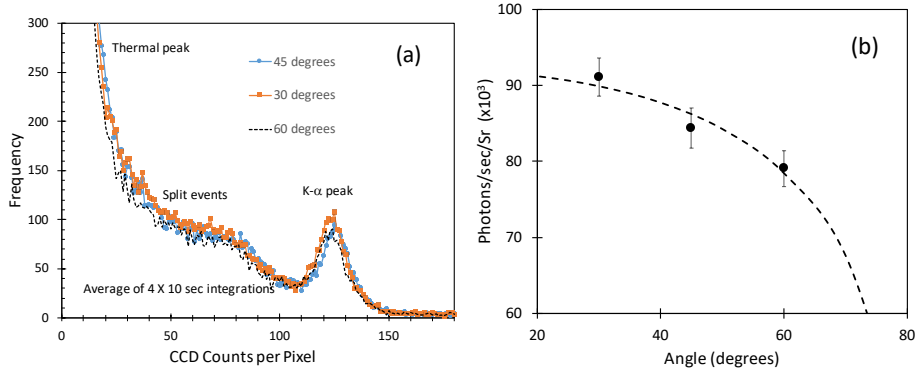
established that the standard deviation in signal level was 0.7% with a maximum excursion from the average of $\sim 1.3\%$. This is well within the overall accuracy of our measurements and stability of the X-ray source is not a principal source of error.

3 Calibration of flat crystals

In this section we present the data for two types of flat Bragg crystal. The first type is HOPG, which is of great utility in Bragg spectrometers for laser plasma X-ray sources. They have a large integrated reflectivity [6, 7] in the regime of a few mrad compared to other typical crystals which have values one or two orders of magnitude lower. This makes them of particular use in X-ray Thomson scattering experiments. A particular feature of their deployment is that in order to maintain good spectral resolution they need to be operated with roughly equal distances from the crystal to the source and detector. This is due to the mosaic spectral focussing effect as discussed in Glenzer *et al* [8]. With this arrangement resolutions of $E/\delta E \sim 1000$ can be readily achieved. The experiment was carried out using the configurations in figure

$$\frac{N_{crys}}{N_{ccd}} = exp(-\alpha_{air}(L_{ccd} - L_{crys}))\frac{\Omega_{crys}}{\Omega_{ccd}} \tag{3.1}$$

where α_{air} is the x-ray absorption coefficient in air and L_{ccd} is the total distance in air from foil to camera in the direct case and L_{crys} for the Bragg crystal case. For the direct case, Ω_{ccd} is the solid angle subtended by the CCD and Ω_{crys} is the effective solid angle for the Bragg crystal case. This latter quantity contains the integrated reflectivity, R_{int}. In our case we can say;

$$\Omega_{crys} = R_{int}\frac{w}{L_{crys}} \tag{3.2}$$

where w is the height of the CCD chip and L_{crys} is the total distance to the chip via the crystal. The ratio of these latter two parameters defines the opening angle of the fan of rays that are intercepted as shown in figure

$$\chi^2 = \sum \frac{(y_i - Y_i)^2}{Y_i} \tag{3.3}$$

where y_i is a data point and Y_i is the fitted value. We fit values from the peak of the K-α at 116 counts/pixel to 135 counts/pixel as this is the region we expect out Gaussian approximation

to be valid in. The error bars for the amplitude and width of our fitted peaks are determined with 95% confidence by varying each independently about the best fit to achieve $\chi^2 = \chi^2_{min} + 4.0$ as described by Hughes and Hase [1]. The resultant error bars in amplitude and width for the direct measurements and the Bragg reflected measurements were combined in quadrature to give an error bar of order 5%. Combined with estimated systematic error due to measurement of distances we estimate our total error bar in reflectivity to be ~ 10%.
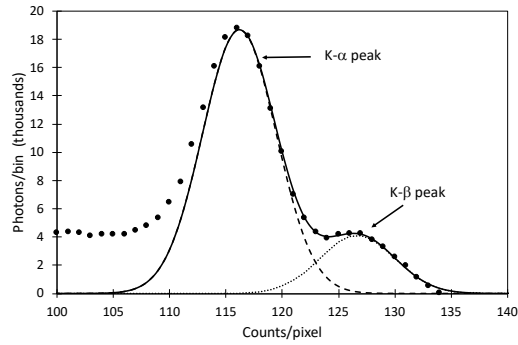
Figure 4. Histogram data for direct detection of the K-shell photons for a Ti foil (closed circles). We can see the peaks due to both K-α (dashed line) and K-β (dotted line) photons fitted to Gaussian curves. The black solid line is the sum of the two Gaussian fits.

For the Bragg crystal case, the data is shown in figure
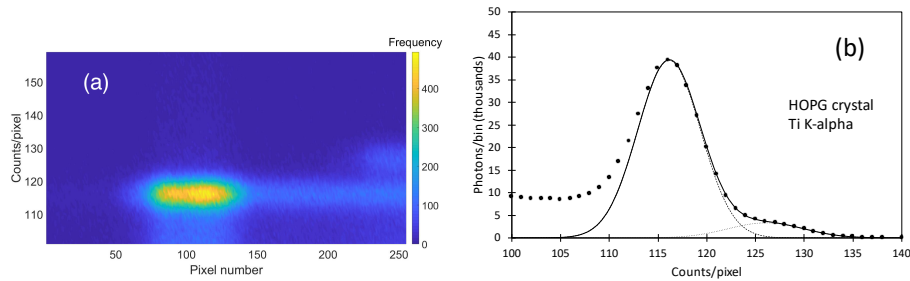
Figure 5. (a) Contour map for Bragg crystal data with a HOPG crystal. We can see the K-β photons are spectrally and spatially shifted as expected and extend off the end of the CCD, thus reducing the relative contribution of the K-β signal, we calculate the relative contribution of the K-β by fitting Gaussians to the data as shown in (b). Histogram for data collected from HOPG crystal with Ti foil. The solid circles are the experimental data, the K-α fit is the dashed line, the K-β fit is the dotted line and the total fit is the solid line.

In the table below, we show the results of measurements using the Kα lines of Ti (4.51 keV) and V (4.95 keV) for a HOPG crystal and a Si (111) crystal. We can see that error bars are in the ~ 10-20 % range, which is sufficient for many applications. For HOPG these results are in the expected range, which can vary according to the manufacture technique e.g. [6]. For Si(111) the results are in between the expected results [9] for a perfect crystal and a mosaic crystal.

Table 1. Summary of reflectivity results for flat crystals.

Crystal	E_{ph} (keV)	R_c (mrad)	error (mrad)	error (%)
HOPG	4.51	1.88	0.18	10
HOPG	4.95	1.87	0.16	9
Si (111)	4.51	0.131	0.014	11
Si (111)	4.95	0.123	0.011	9

4 Curved crystals

We have applied the technique described above to a curved HOPG crystal in the Von-Hamos configuration. For the purposes of this work, we placed the CCD detector surface normal to the X-rays coming from the crystal to make for easier alignment. The method is the same as for flat crystals except that the effective solid angle for the measurements from the crystal is given by;

$$\Omega_{crys} = R_{int} \frac{w_{crys}}{(L_{cry}/2)} \tag{4.1}$$

where w_{crys} is the width of the crystal along the curved direction and the factor of 2 appears because the it is the distance from source to crystal alone that is needed. In our case the curved HOPG crystals are 30 mm long and 20 mm wide along the direction that is curved (radius, R = 50 mm). They are manufactured by coating $\sim$ 100 μm of HOPG onto a glass substrate. The distance from source to ccd is determined by the focussing distance for the appropriate Bragg angle; L_{crys} = 2R/sin(θ_B) = 244 mm for the Ti K-α case. We have measured the integrated reflectivity for two such crystals and the results are summarised in the table below.

Table 2. Reflectivity results for Von-Hamos type HOPG crystals.

Crystal	E_{ph} (keV)	R_c (mrad)	error (mrad)	error (%)
VH HOPG A	4.51	2.56	0.14	5
VH HOPG B	4.51	2.37	0.14	6

5 Conclusions

In this paper we have described a relatively straightforward method for absolute calibration of the reflectivity of Bragg crystals used in X-ray plasma spectroscopy. The most expensive item is the 16-bit X-ray CCD used for photon counting. The signal measurement method is the same in both the direct and crystal reflection measurements, meaning that the absolute quantum efficiency of the detector does not need to be known as it is the same in both cases. The high reflectivity of HOPG crystals has allowed us to obtain data with error bars better that 10% for the curved crystals aided perhaps by the much shorter total integration times made possible by the focusing geometry that enhanced the effective solid angle. For the flat crystals, although smaller errors have been obtained with a double crystal technique [1] but our errors in the range $\sim$ 10% are small enough to be useful still and could in principle be improved up by taking a longer time to collect the data.

Acknowledgments

References

[1] V.A. Boiko, A.Y. Faenov and S.A. Pikuz *X-ray spectroscopy of multiply charged ions from laser plasmas*, *J. Quant. Spectrosc. Radiat. Transfer* **19** (1985) pp. 11-50

[2] J.D. Kilkenny, R.W. Lee, M.H. Key and J.G. Lunney, *X-ray spectroscopic diagnosis of laser-produced plasmas, with emphasis on line broadening*, *Phys. Rev. A.* **22** (1980) pp. 2746-2760

[3] R.J. Hutcheon, L. Cooke, M.H. Key, C.L.S. Lewis and G. Bromage, *Neon-Like and Fluorine-Like X-ray Emission Spectra for Elements Cu to Sr*, *Physica Scripta* **21** (1980) pp. 89-97

[4] R.P. Kraft *et al* , *Measuring the soft x-ray quantum efficiency of charge coupled devices using continuum synchrotron radiation Nucl. Instr. and Meth. in Phys. Res. A*, **366**, (1995) pp. 192-202

[5] J. H. Scofield, *Exchange corrections of K x-ray emission rates*, *Phys. Rev. A* **9** (1974) pp. 1041-1049

[6] H. Legall, H. Stiel, V. Arkadiev and A.A. Bjeoumikhov *High spectral resolution x-ray optics with highly oriented pyrolytic graphite*, *Optics Express* **14** (2006) pp. 4570-4576

[7] M. Sanchez del Rio *et al* , *Focusing properties of mosaic crystals SPIE proc.*, **3448**, (1998) pp. 246-255

[8] S.H. Glenzer and R Redmer, *X-ray Thomson scattering in high energy density plasmas Rev. Mod. Phys.*, **81**, (2009) pp. 1625-1663

[9] B.L Henke, E.M Gullikson and J.C. Davis, *X-ray interactions: Photoabsorption, scattering, transmission and reflection at E=50-30,000 eV, Z=1-92, Atomic Data abd Nuclear Data Tables*, **54** (1993), pp 181-342

[10] I.G. Hughes and T.P.A. Hase *Measurements and their uncertainties, Oxford University Press, 2010*

[11] U. Zastrau and E. Frster *Integrated reflectivity measurements of hydrogen phthalate crystals for high-resolution soft x-ray spectroscopy*, *Journal of Instrumentation*, **9** (2014), p09008